

# NOVEL APPROACHES IN MODELING SURFACE NMR SIGNALS FOR HYDROGEOLOGICAL APPLICATIONS

Marian Hertrich, Jochen Lehmann-Horn, Jan Walbrecker, and Hendrik Schulz

ETH Zürich, Institute of Geophysics  
Sonneggstr. 5, 8092 Zürich, Switzerland  
e-mail: hertrich@aug.ig.erdw.ethz.ch, web page: <http://www.aug.geophys.ethz.ch>

**Key words:** surface nuclear magnetic resonance, groundwater, geophysics, inversion

**Summary.** Surface nuclear magnetic resonance (NMR) takes advantage of precession phenomena that result from exciting spin magnetic moments of groundwater hydrogen protons using magnetic fields generated by a large surface loop. The method allows subsurface water content to be determined from inversions of measurements of a single surface loop in 1-D mode (magnetic resonance soundings, MRS) or from a series of coincident and/or offset transmitter and receiver loops in 2-D mode (magnetic resonance tomography, MRT). Until recently, computational approaches have been restricted to simplified models that are not able to explore the full information content of the recorded signals or are inappropriate for complex topography or subsurface structures. Major oversimplifications include computations of spin dynamics that are based on incomplete descriptions of double-pulse sequences or assumptions of (a) regularly shaped surface loops on a flat earth, (b) a 1-D subsurface resistivity distribution, or (c) ideal excitation pulses in terms of duration, time-domain shape and carrier frequency.

We present recent innovations in more flexible and accurate computation of surface NMR signals approaches to significantly extend the applicability of surface NMR towards faster and more accurate modelling, surveys in rugged terrain and estimates of unbiased relaxation constants to potentially predict key hydrological parameters from surface NMR measurements.

## 1 PRINCIPLES OF SURFACE NMR

Exploration for groundwater using surface NMR takes advantage of the spin magnetic moments of protons in hydrogen atoms that precess around the earth's static magnetic field  $\mathbf{B}_0$  at the Larmor frequency  $\omega_L$ , given by

$$\omega_L = \gamma |\mathbf{B}_0|, \quad (1)$$

where  $\gamma$  is the gyromagnetic ratio. As a consequence of thermally induced interactions between the water molecules, the ensemble of spin-magnetic-moment vectors gains a slight

bias that results in a small net magnetization  $\mathbf{M}_0$  that is proportional to the water content and parallel and proportional to  $\mathbf{B}_0$ . For a surface NMR experiment, a short pulse of strong current alternating at the Larmor frequency is passed through a large surface loop (radius ranging from 5 to 150m) and the generated electromagnetic field perturbs the spin magnetic moments of hydrogen protons. After pulse cut-off, the spins precess around the ambient field, exponentially releasing their excess energy, generating a small but perceptible electromagnetic signal that can be picked up by receiver loops. Progressively deeper regions of the subsurface are probed by increasing the pulse moment

$$q = I_0\tau, \quad (2)$$

where  $I_0$  is the current through the coil and  $\tau_p$  is the duration of the pulse. The initial amplitude of the response signal after termination of the pulse is given by [1]

$$V(q) = 2\omega_L M_0 \int_{vol} f(\mathbf{r}) \left| \mathbf{B}_{\perp}^{-}(\mathbf{r}) \right| e^{2i\zeta(\mathbf{r})} M_{\perp}(\mathbf{r}) d^3r, \quad (3)$$

where  $M_0$  is the equilibrium magnetization of hydrogen protons and the integral represents the superposition of signals generated by the precessing spin magnetic moments. In the integral, (i)  $f(\mathbf{r})$  is the amount of water at location  $\mathbf{r}$ , which scales the response of each volume element by the number of hydrogen nuclei within it, (ii)  $\mathbf{B}_{\perp}^{-}$  is the counter-rotating component of the alternating electromagnetic field normalized for unit currents in the coil, (iii)  $\zeta(\mathbf{r})$  are phase lags associated with the distances between the coil and points  $\mathbf{r}$  in a lossy subsurface and (iv)  $M_{\perp}(\mathbf{r})$  is a measure of the NMR signal induced at point  $\mathbf{r}$ . Eq. (1) can be expressed as

$$V(q) = \int_{vol} f(\mathbf{r}) K(q, \mathbf{r}) d^3r, \quad (4)$$

with  $f(\mathbf{r})$  the water content as the dependent parameter and  $K$  the integral kernel that accounts for the measurement-configuration information, attributes of the local Earth magnetic field, subsurface resistivity distribution and various constants.

## 2 DISCRETISATION AND VOLUME INTEGRATION

Approximating the continuous volume integration by summation over piecewise constant water contents and magnetic fields leads to the matrix notation

$$\mathbf{V} = \mathbf{Kf}. \quad (5)$$

Depending on the dimension of the survey, the water content distribution can be considered to be 1-D, 2-D or 3-D. Independent of the dimension of the water content distribution, the surface-NMR integral must be solved in 3-D and integrated/summed over each water content parameter cell. The spatial discretisation of the NMR-kernel required to provide sufficient accuracy strongly depends on the gradient of the highly inhomogeneous loop

magnetic fields across each parameter cell. In high gradient regions a very fine discretisation is required, whereas low gradient regions may be accurately represented by relatively coarse discretisation.

To obtain appropriate levels of discretisation, we have developed a hierarchical meshing scheme [2]. In a first step, a parameter mesh is created that accounts for (i) model resolution, such that parameter-element sizes reflect the available resolution of the survey, (ii) surface topography, which can have an important influence on the accuracy of the numerically computed signals and (iii) subsurface topology, which allows the introduction of à priori information in the model, in the form of known fixed boundaries, to help constrain the inverse problem. In a second step, the 1-D and 2-D elements are expanded into 3-D (Figure 1b-1c) and the resulting volumes meshed at appropriate sizes to allow accurate numerical computations of the NMR kernel (Figure 1d). In a final step, the kernels are summed over the parameter volume using linear elements (Figure 1e).

### 3 COMPUTATION OF THE LOOP MAGNETIC FIELD

The spatial distribution of the loop magnetic fields  $\mathbf{B}(\mathbf{r})$  needs to be computed accurately to predict surface NMR signals according to Equation (3). Sufficiently accurate solutions exist for simple loop shapes (circular, rectangular) and idealized subsurface resistivity distributions (homogeneous or 1-D stratified earth [3]). For loops placed on rugged terrain and/or for complex subsurface resistivity distributions numerical approaches must be employed. For these cases we have developed efficient algorithms that include: (i) thin wire integral-equation approximations (IE) for representing shaped loops (including topography) situated on resistive subsurfaces, (ii) boundary integral (BI) techniques for limited conductive structures situated in a resistive host rock and (iii) finite element methods (FEM) for arbitrary resistivity distributions.

Since pure FEM techniques may be computationally expensive, we have developed hybrid IE/FEM and BI/FEM solutions to provide accurate magnetic field distributions using practical amounts of computational memory [4]. For the computation of surface NMR signals, the subsurface resistivity distribution should be known from supplementary resistivity surveys.

Figure 2 shows an example of the computed electromagnetic field (intensity and direction in Figure 2a) and the surface NMR kernel function (Figure 2b) for a 100x100m surface loop located on rugged resistive ground. We have recently demonstrated that our new approach yields accurate 2-D water content tomograms for a terminal moraine with substantial topography and difficult surface conditions [5].

### 4 SPIN DYNAMICS FOR SURFACE NMR CONDITIONS

An NMR data set is usually analyzed in terms of the initial amplitudes and the relaxation times. Initial amplitudes are related to the amount of water in the investigated volume, whereas the relaxation times may be interpreted in terms of pore space properties [6]. To

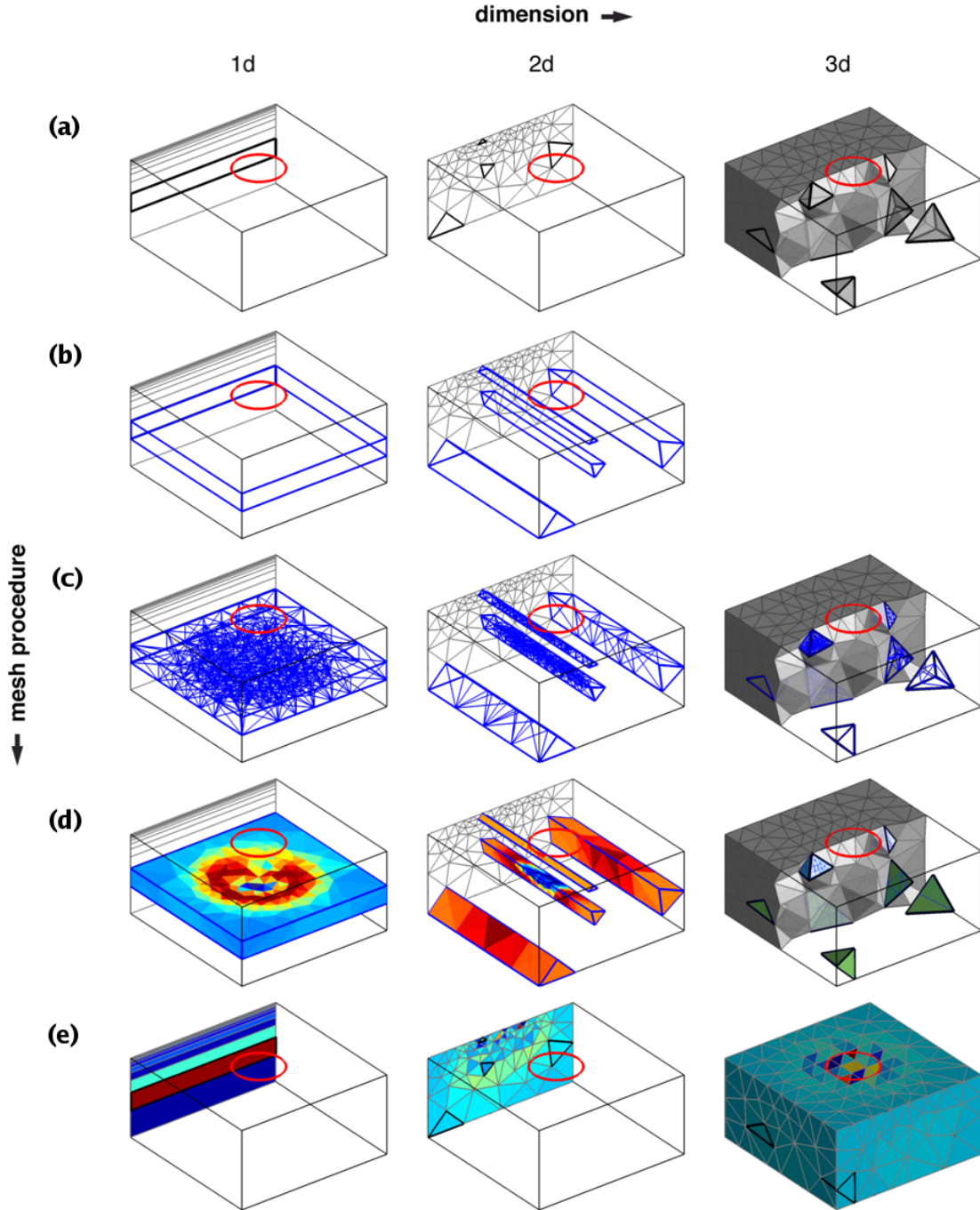


Figure 1: Hierarchical meshes in one (1-D), two (2-D) and three (3-D) dimensions. Steps (a) - (e) represent the main mesh generation steps (a) parameter mesh, (b) expansion of the single elements (1-D and 2-D), (c) adaptive element refinement, (d) sensitivity calculation and (e) reduction to the original parameter mesh by integration or summation. The expansion step (b) is not necessary in 3-D.

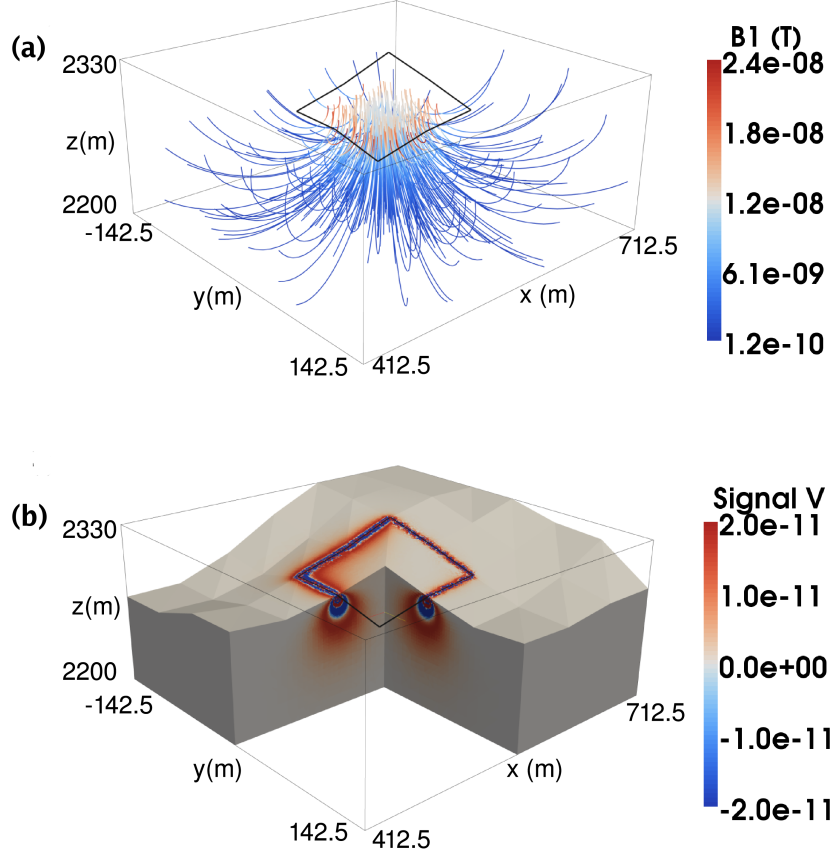


Figure 2: Spatial distribution of (a) the loop magnetic field intensity (color coded) and direction (streamlines) and (b) surface NMR kernel for a 100x100 m loop on rugged terrain.

interpret observed NMR signals correctly the experimental conditions must be described as accurately as possible.

The NMR response  $M_{\perp}$  of each volume element ( $\mathbf{r}$ ) in Equation (3) is given by solving the Bloch equations

$$\frac{\partial}{\partial t} \mathbf{M}(t) = \gamma \mathbf{M}(t) \times (\mathbf{B}_0 + \mathbf{B}_{\perp}^+(t)) - \frac{M_x(t) \hat{\mathbf{x}}}{T_2^*} - \frac{M_y(t) \hat{\mathbf{y}}}{T_2^*} - \frac{(M_z(t) - M_0) \hat{\mathbf{z}}}{T_1}, \quad (6)$$

where  $\mathbf{B}_0$  and  $\mathbf{B}_{\perp}^+$  are the static and loop magnetic fields,  $\hat{\mathbf{x}}$ ,  $\hat{\mathbf{y}}$  and  $\hat{\mathbf{z}}$  are the Cartesian unit direction vectors and  $T_2^*$  and  $T_1$  are the transverse and longitudinal relaxation constants. Under ideal conditions in which pulses are short compared to the shortest relaxation time and there is a perfectly matched Larmor frequency, the solution of the Bloch equations is

$$M = \sin(\gamma q B_{\perp}). \quad (7)$$

Equation (7) is the solution most widely used in conventional NMR applications in which

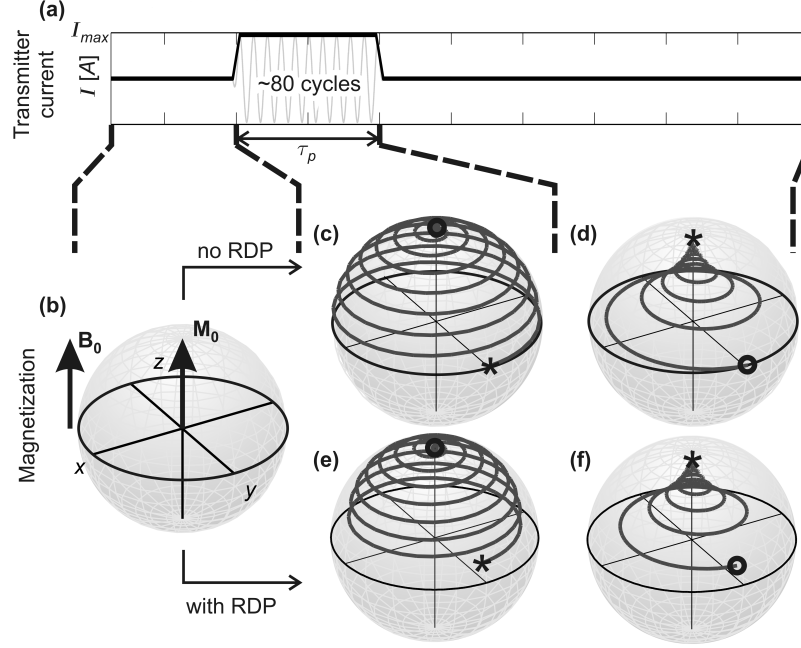


Figure 3: (a) Current  $I$  in a transmitter coil produces a  $\pi/2$  pulse of secondary alternating magnetic field  $B_1$ . Light gray line: sketch of the alternating current; black line: current envelope. (b) Primary static magnetic field direction  $B_0$  and parallel macroscopic magnetization  $M_0$  representing the ensemble of spin-magnetic-moment vectors in thermal equilibrium. (c, d) Trajectories of magnetization during and after activation of pulse  $B_1$  assuming negligible RDP. Circle: start point; star: end point. (e, f) Trajectories of magnetization as for (c) and (d) but including the effects of RDP

experimental settings under laboratory conditions can be accurately adjusted. In surface NMR, where (i) relatively long pulses are required to excite spins in relevant depths and (ii) the static earth magnetic field is usually subjected to temporal variations that result in frequency offsets of Larmor and excitation frequency, numerical solutions of the Bloch equations are required for accurate modeling of the NMR response.

We have implemented a forth-order Runge-Kutta algorithm with self adaptive step sizes to study the range of validity of the conventional sine approximation in Equation 7. We found that for a wide range of relaxation times typical of sedimentary host rocks, relaxation-effects during the pulse (RDP) may be substantial, resulting in biased estimates of water content and relaxation constants. We have proposed relatively simple interpretational approaches that can reduce RDP-related errors to less than 2% [7].

Figure 3 shows a comparison of the excitation process for an NMR experiment (i) under idealized conditions of a 'short' pulse, neglecting RDP effects (Figure 3c and d) and (ii) with RDP-effects taking place (Figure 3e and f).

## 5 INVERSION

To estimate subsurface water content soundings (1-D) or tomograms (2-D/3-D) are required. For this, the observed data need to be inverted. To minimize the misfit of observed and model predicted data and at the same time apply constraints to the model the guarantee the 'simplest' possible water content distribution, we employ an iterative solver of the Gauss-Newton system of equations:

$$\Delta \mathbf{f}^l = \left( \mathbf{K}^T \mathbf{C}_d^{-1} \mathbf{K} + \lambda \mathbf{C}_m^{-1} \right) \left( \mathbf{K}^T \mathbf{C}_d^{-1} \left( \mathbf{v} - \mathbf{K} \mathbf{f}^{l-1} \right) - \lambda \mathbf{C}_m^{-1} \mathbf{f}^{l-1} \right), \quad (8)$$

where  $\Delta \mathbf{f}^l$  is the model update of l-th iteration,  $\lambda$  is the regularization parameter and  $\mathbf{C}_m^{-1}$  and  $\mathbf{C}_d^{-1}$  are the model and data covariances, respectively. One-dimensional inversion schemes for single coincident-transmitter loop measurements were introduced at early stages in the development of surface NMR systems [8]. Major advances in inversion techniques now allow us to reconstruct 2-D water bearing bodies from a series of measurements along a profile. The resolution of relatively small shallow anomalies can be substantially improved by employing multi-offset measurements [9]. Conventional inversion schemes require the water content changes to be smooth across the model. As a consequence, gradational changes are reconstructed for water content distributions that are, in reality, abrupt (i.e., at geological boundaries). In cases in which the boundaries are well-defined from supplementary geophysical methods (e.g., seismics or ground penetrating radar) or a priori geological information, the boundaries can be incorporated in the inversion process to provide a significantly improved reconstruction of subsurface water-content distributions (Figure 4).

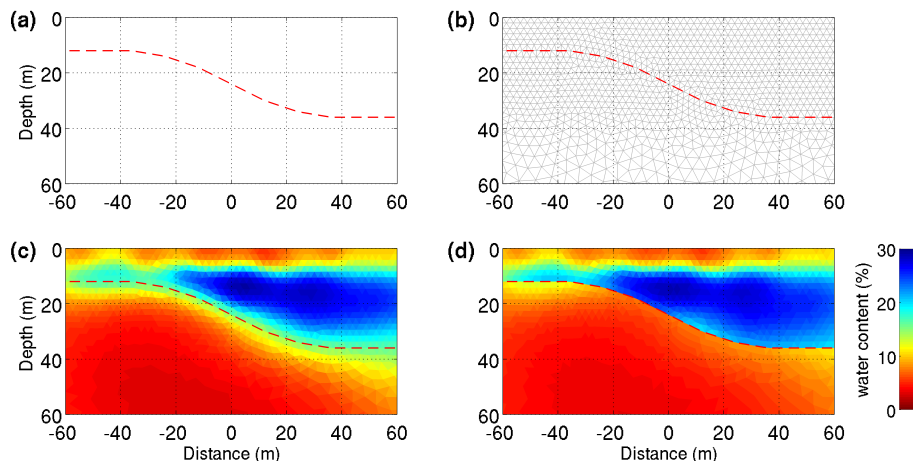


Figure 4: Synthetic example of a shallow aquifer model with (a) the lower boundary known a priori, (b) the parameter mesh created with the boundary included, (c) the inversion result with the same smoothness constraints across the entire domain and (d) with the smoothness constraints across the boundary reduced to 25%

## 6 CONCLUSION

Considering humanity's increasing interest in groundwater resources, surface NMR has the potential to provide important parameters for subsurface characterization. Conventional approaches of surface NMR modeling and inversion are based on assumptions that are not necessarily fulfilled for applications in real experimental conditions and geologic environments. With more sophisticated approaches in modeling the loop magnetic fields and NMR spin dynamics and advanced schemes of mesh generation and data inversion, we have developed solutions that provide improved estimates of NMR-parameters.

## REFERENCES

- [1] M. Hertrich, Imaging of groundwater with nuclear magnetic resonance, *Progress in Nuclear Magnetic Resonance Spectroscopy* 541 (2008) 227–248.
- [2] H. Schulz, J. Lehmann-Horn, M. Hertrich, Hierarchical meshes for surface nuclear magnetic resonance modelling, in: *Proceedings of the 4th International Workshop on MRS, Grenoble, France, 2009*, pp. 195–200.
- [3] S. H. Ward, G. W. Hohmann, Electromagnetic theory for geophysical applications, in: M. N. Nabighian (Ed.), *Electromagnetic methods in applied geophysics, Vol. 1 of Investigations in Geophysics, Soc. Expl. Geophys.*, 1988, Ch. 4, pp. 131–311.
- [4] J. Lehmann-Horn, M. Hertrich, A. G. Green, Hybrid electromagnetic modeling of large nmr surface loops on rugged terrain, in: *Proceedings of the 4th International Workshop on MRS, Grenoble, France, 2009*, pp. 129–134.
- [5] J. Lehmann-Horn, J. Walbrecker, M. Hertrich, G. Langston, Initial results of a surface-nmr survey to assess water storage capacity of a terminal moraine in yoho national park (BC, Canada), in: *Proceedings of the 4th International Workshop on MRS, Grenoble, France, 2009*, pp. 125–128.
- [6] W. E. Kenyon, Petrophysical principles of applications of NMR logging, *The Log Analyst* (1997) 21–43.
- [7] J. O. Walbrecker, M. Hertrich, A. G. Green, Accounting for relaxation processes during the pulse in surface NMR data, *Geophysics* 74 (6) (2009) G27–G34.
- [8] A. Legchenko, O. Shushakov, Inversion of surface NMR data, *Geophysics* 63 (1) (1998) 75–84.
- [9] M. Hertrich, A. G. Green, M. Braun, U. Yaramanci, High-resolution surface nmr tomography of shallow aquifers based on multioffset measurements, *Geophysics* 74 (6) (2009) G47–G59.